Available online at www.sciencedirect.com
ScienceDirect
Journal of Power Sources 170 (2007) 395–400
JOURNAL OF POWER SOURCES
www.elsevier.com/locate/jpowsour

Short communication

Novel alkaline earth silicate sealing glass for SOFC Part II. Sealing and interfacial microstructure

Yeong-Shyung Chou [a,*], Jeffry W. Stevenson [a], Robert N. Gow [b]

[a] *Pacific Northwest National Laboratory, Richland, WA 99354, United States*
[b] *Office of Science, Community College Institute, Montana Tech, MT 59701, United States*

Received 12 February 2007; received in revised form 21 March 2007; accepted 29 March 2007
Available online 10 April 2007

Abstract

This is the second part of a study of a novel Sr–Ca–Ni–Y–B silicate sealing glass for solid oxide fuel cells (SOFC). Part I of the study addresses the effect of NiO on glass forming, thermal, and mechanical properties, and is presented in the preceding paper. In this paper (part II), candidate composite glass with 10 vol.% NiO was tested for sealing standard coupons of Ni/YSZ anode-supported YSZ electrolyte bilayer and metallic interconnect Crofer22APU at various temperatures. Samples sealed at the highest temperature (1050 °C) showed hermetic seal after fully reduction and 10 thermal cycles. The interfacial microstructure characterization showed no distinct reactions at the interfaces of glass/YSZ or glass/metal, though some segregation of Ni was found along the glass/metal interface. Possible reactions were discussed. Overall the composite glass with 10 vol.% NiO appeared to be a good candidate for SOFC sealing.

Keywords: Glass seal; SOFC; Leak rate; Interface; Composite

1. Introduction

Solid oxide fuel cells (SOFCs) are emerging technologies which can provide clean and high efficiency energies as compared to the conventional combustion technologies [1]. As mentioned in the previous paper [2] that many technical hurdles are still present and must be solved before the technology could advance. One of the many challenges is the development of a reliable and robust sealant or sealants. The harsh SOFC operation conditions of elevated temperatures (~750–1000 °C), oxidizing, reducing, and moist environment, electrical loading, and thermal stresses from transient or steady-state operations have put great constraints in seal development. And the complex nature of multiple sealing sections between similar and/or dissimilar materials of a planar SOFC stack with internal manifolding would also limit the choices for sealants. Candidate sealant or sealants must show the desired hermeticity or allowable leak rates, and thermal, mechanical, electrical, and chemical stability in the harsh SOFC operating conditions for a lifetime up to 40,000 h and numerous thermal cycles [2].

To date, there are three approaches for SOFC seal development: glass/glass–ceramic seals [3–11], mica-based compressive seals [2,12,13], and metallic brazes [14–16]. In this work, a Sr-silicate based glass was chosen as the candidate sealing material, due to good match in coefficients of thermal expansion (CTE) and potential long-term stability in thermal, electrical, and chemical properties. Currently, alkaline earth based aluminosilicate glasses have been developed and extensively studied as the candidate sealing glasses [4–9,11,17]. However, most studies were focused on crystallization kinetics and the influence of different nucleating agents [8], the thermal and chemical stability [5,9], and thermal cycle stability [10]. Few have looked into the interfacial reactions or chemical compatibility at the glass/metal and/or glass/YSZ interfaces. Yang et al reported a yellowish interfacial compound ($BaCrO_4$) was formed at the metal/glass interface at cathode side near the outer edge [18], but not at the anode metal/glass interface. The favorable formation of $BaCrO_4$ at cathode side was also consistent with thermodynamic calculations. Haanappel et al. evaluated the interfacial reaction of several Ba–Ca-silicate sealing glasses on various metallic interconnects under DC load and

* Corresponding author at: K2-44, PNNL, P.O. Box 999, Richland, WA 99354, United States. Tel.: +1 509 3752527; fax: +1 509 3752186.
E-mail address: yeong-shyung.chou@pnl.gov (Y.-S. Chou).

0378-7753/$ – see front matter © 2007 Published by Elsevier B.V.
doi:10.1016/j.jpowsour.2007.03.060

simulated SOFC environments. They found excessive internal Cr-oxidation of ferritic steels accompanied by external conducting Fe-oxide formation, only occurred for glass containing small amount of PbO [19]. The internal oxidation resulted in volume change and eventually led to the crack formation of glass seal.

In the preceding paper, we have investigated the glass forming, thermal, and mechanical properties of a Sr–Ca-silicate sealing glass with various amount of NiO [20]. And two forming processes were tested: glass-making and composite approach. Only the composite approach resulted in sealing glass (YSO-15) with the closest CTE ($12.01 \times 10^{-6}\,^{\circ}C^{-1}$) match SOFC components. The development of these "refractory" sealing glasses with higher (e.g., $\geq$950 °C) sealing temperatures was targeted for the long-term stability as compared to the "standard" sealing glass (e.g., G18) with a sealing temperature $\leq$850 °C for SOFCs to be operated at ~800 °C. The objective of the second part of the work was to investigate the sealing behavior of this particular composite glass at various sealing temperature and the interfacial reactions at both the glass/YSZ and glass/metal interfaces.

2. Experimental

2.1. Coupon sealing and leak test

A composite glass with 10 vol.% NiO (glass YSO-15) was used for coupon sealing and leak tests. This composite glass was made by mixing YSO-1 glass powders with NiO powders at 10 vol.% in *iso*-propanol. Glass YSO-1 was a Sr–Ca–Y–B–Si glass made by melting constituent oxides. Details of the chemical composition, glass making, and composite powder processing were given in Part I of the paper [20]. The composite powders were made into tapes by conventional tape casting method using organic solvents. Coupon sealing was conducted by sandwiching a green glass tape (23 mm × 23 mm) between a Crofer22APU square (25 mm × 25 mm) with a central hole and an anode-supported (YSZ–NiO) thin electrolyte (8YSZ) bilayer (20 mm × 20 mm) as shown in Fig. 1. Crofer22APU (Thyssenkrupp VDM, Michigan) is a ferritic stainless steel with about 20–24 wt.% Cr, and is considered a leading candidate as metallic interconnect for SOFC applications. Typical chemical composition of Crofer22APU is listed in Table 1. The seal sandwich assembly was then placed in a vertical tube furnace and was pressed at ~5 psi during the sealing process. The samples were first slowly heated to 550 °C for binder burn-off. They were then heated to various sealing temperatures of 950 °C, 1000 °C, or 1050 °C for 2 h, followed by heat-treatment (crystallization) at 800 °C for 4 h. For each sealing temperature four duplicate samples were made. After sealing, the sealed coupons were subjected to leak test with ultra-high purity helium at a differential pressure of 4 kPa (~0.4 psi). A small swagelock pipe fitting was pressed against the sealed coupon on the holed surface with vacuum grease. The swagelock fitting was then connected to a reservoir of known volume and a pressure transducer. The room temperature leak rates were determined from the change of pressure versus time using a data acquisition/switch unit (Mod # 34970A, Agilent, CA) over a 5 min period. The system (background) leak rates were determined using plain crofer square without glass and central hole. The details of the leak setup and the calculation of the leak rates are given in Refs. [2,11]. The coupons sealed at 1050 °C were then reduced in a flowing gas of 70% H_2/30%H_2O at 800 °C for 24 h, followed by 10 thermal cycles between ~50 °C and 800 °C in the same atmosphere. After 10 thermal cycles, the samples were cooled down and leak tested again.

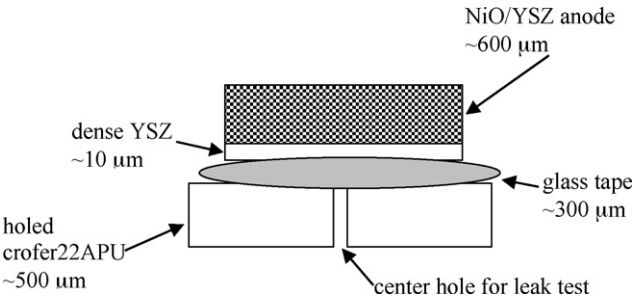

Fig. 1. Schematic drawing shows the assembly of coupon sealing.

2.2. Interfacial characterization

After leak testing the sealed coupons were prepared for interfacial characterization. The samples were cut, mounted, ground, and polished with diamond paste of 1–3 μm as the final finish. The polished samples were then coated with carbon and examined by a scanning electron microscopy equipped with energy dispersive spectroscopy (JOEL, JSM-5900LV).

3. Results and discussion

3.1. Effect of sealing temperature on coupon sealing

As shown in earlier paper that the composite approach yielded better CTE matching than the glass making approach when NiO was introduced into the Sr–Ca–Y–B–Si glass system. And composite glass YSO-15 was selected for coupon sealing and leak tests due to matching CTE ($12.01 \times 10^{-6}\,^{\circ}C^{-1}$) and appropriate amount of NiO (10 vol.%). Composite glass YSO-16 had a higher CTE ($12.16 \times 10^{-6}\,^{\circ}C^{-1}$); however, it contained

Table 1
Typical chemical composition of Crofer22APU

	Cr	Fe	C	Mn	Si	Cu	Al	S	P	Ti	La
Min.	20.0	Bal.		0.30						0.03	0.04
Max.	24.0	Bal.	0.03	0.80	0.50	0.50	0.50	0.020	0.050	0.20	0.20

Data from Materials Data Sheet #4046, Thyssenkrupp VDM.

Table 2
Room temperature leak rate (in sccm cm^{-1}) for composite glass (YSO-15, 10 vol.% NiO) before and after 10 thermal cycles in reducing environment

Sample no.	Sealing cond.	Leakage, as-sealed	Leakage, after cycling
1	950 °C/2 h	2.7E−01	
2	950 °C/2 h	8.8E−02	
3	950 °C/2 h	1.5E−02	
4	950 °C/2 h	4.0E−04	
5	1000 °C/2 h	4.1E−04	
6	1000 °C/2 h	9.1E−03	
7	1000 °C/2 h	3.0E−03	
8	1000 °C/2 h	2.9E−03	
9	1050 °C/2 h	3.9E−04	1.0E−04
10	1050 °C/2 h	1.0E−04	2.0E−04
11	1050 °C/2 h	4.0E−04	1.0E−04
12	1050 °C/2 h	2.9E−04	1.0E−04

15 vol.% of NiO which was close to the percolation limit and therefore not selected. Four duplicate coupon pairs were sealed at three different temperatures of 950 °C, 1000 °C, and 1050 °C in air. After sealing, the glasses on the samples showed different colors depending on the sealing temperature: green for 950 °C, light brown for 1000 °C, and black for 1050 °C. The darker color for higher sealing temperature was likely due to more severe reaction of composite glass with Cr, Fe, and Mn from the Crofer22APU, which were known to form a Cr-rich oxide layer and a thin Mn-Cr spinel oxide outer layer over the time. Nevertheless, all sealed coupons had sufficient bond strength to resist being pulled apart by hand. The results of room temperature leakage tests are listed in Table 2. The leak test system was first measured without samples to determine the background (system) leakage, which was found to be $\sim 5.0 \times 10^{-4}$ sccm cm^{-1} (standard cubic centimeter per minute per centimeter of leak length). Samples sealed at 950 °C were not hermetic (except sample #4) with leakage in the range of 10^{-1} to 10^{-2} sccm cm^{-1}. Leakage of 10^{-1} sccm cm^{-1} or higher often resulted from brittle fracture of the rigid glass seal or the ceramic parts (anode support or dense electrolyte). Leak rates of 10^{-2} sccm cm^{-1} were similar to compressive hybrid mica seals [12,13]. Leakage of this order would likely have a minor effect on the electrochemical performance; however, it could have a significant impact on the structural integrity of the stack, depending on the types of seal. For compressive mica seals, the fuel leaked through the open channel or interstitial between discrete mica flakes and the leakage was therefore fairly uniform along the seal periphery. The diffuse fuel combustion from this type of leak would be expected to have much less impact on the structural degradation than a single crack or defect of conventional rigid glass seals. This is because excessive local heating/burning could occur and the crack opening can continue to grow and eventually lead to stack failure. Samples sealed at 1000 °C showed leakage close to hermetic seals with three samples in the $(3–9) \times 10^{-3}$ sccm cm^{-1} range. Samples sealed at 1050 °C had the lowest leakage, with all 4 samples showing a hermetic seal, i.e., leak rates equivalent to or smaller than the background leakage. The parent glass (YSO-1, i.e., no NiO) was found to be hermetic when sealed at 950–1000 °C. Adding the inert NiO particles likely would require higher temperatures for hermetic sealing as observed in this study.

After leak testing, the coupons sealed at 1050 °C were selected for reduction tests which involved exposure to a wet reducing environment (30% H_2O/70% H_2) followed by 10 thermal cycles in the same environment. After reduction and thermal cycling, the samples were again leak tested at room temperature. The results showed hermetic for all four samples with leakage in the range of $\sim(1–2) \times 10^{-4}$ sccm cm^{-1} (Table 2).

3.2. Interfacial characterization of as-sealed coupons along metal/glass interface

Both the as-sealed and the reduced coupons were subjected to microstructure and interfacial characterization. The microstructures of glass/metal and glass/YSZ interface of the as-sealed coupon are shown in Figs. 2–4 for samples sealed at 950 °C, 1000 °C, and 1050 °C, respectively. For comparison, single Crofer22APU and YSZ electrolyte samples without sealing glass were also fired with the same heat-treatment and the microstructures are shown in Fig. 5. Crofer22APU is a ferritic stainless steel which contains ∼22% Cr. It's chosen in this study as metallic interconnect because it forms a continuous conductive chromia-based oxide scale in air and has a matching CTE with NiO/YSZ anode-supported cells.

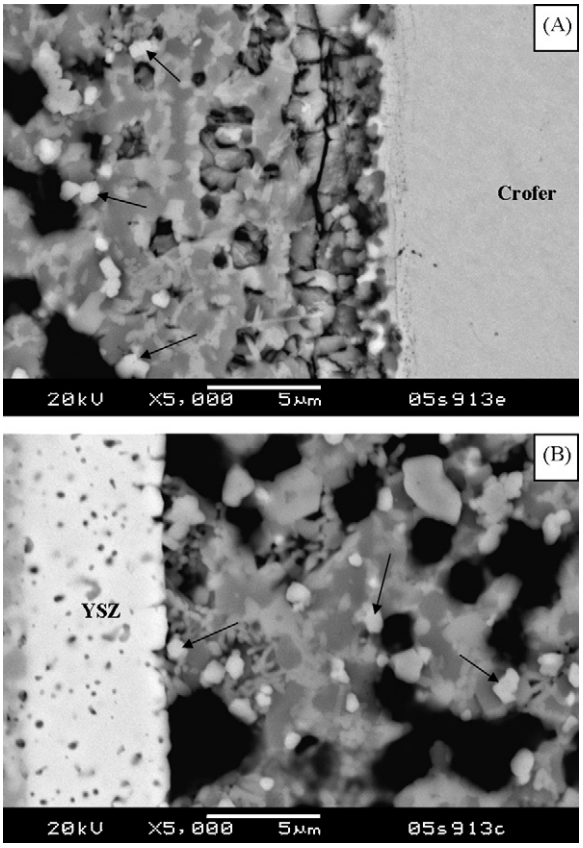

Fig. 2. Interfacial microstructure of composite glass (YSO-15) sealed at 950 °C/2 h at (A) Crofer metal and (B) YSZ electrolyte interface. White particles are NiO (arrows).

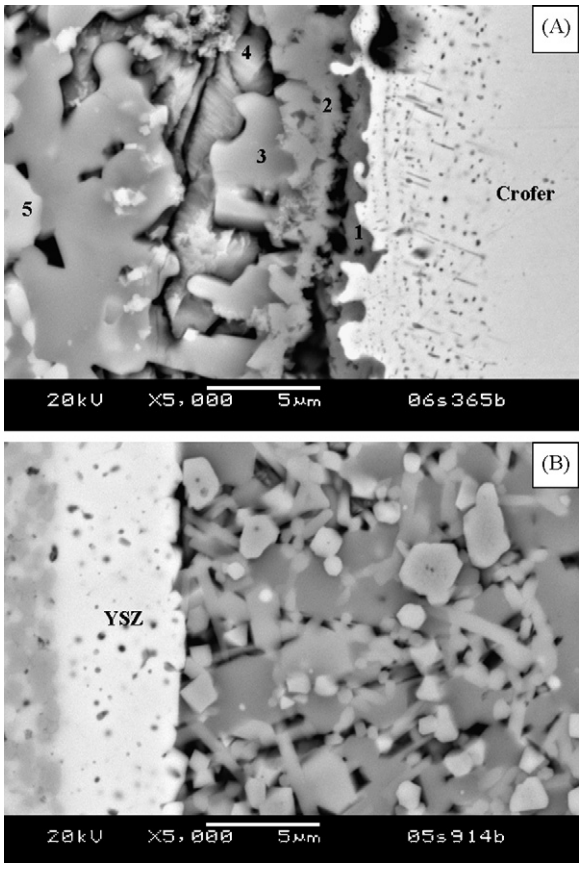

Fig. 3. Interfacial microstructure of composite glass (YSO-15) sealed at 1000 °C/2 h at (A) Crofer metal and (B) YSZ electrolyte interface.

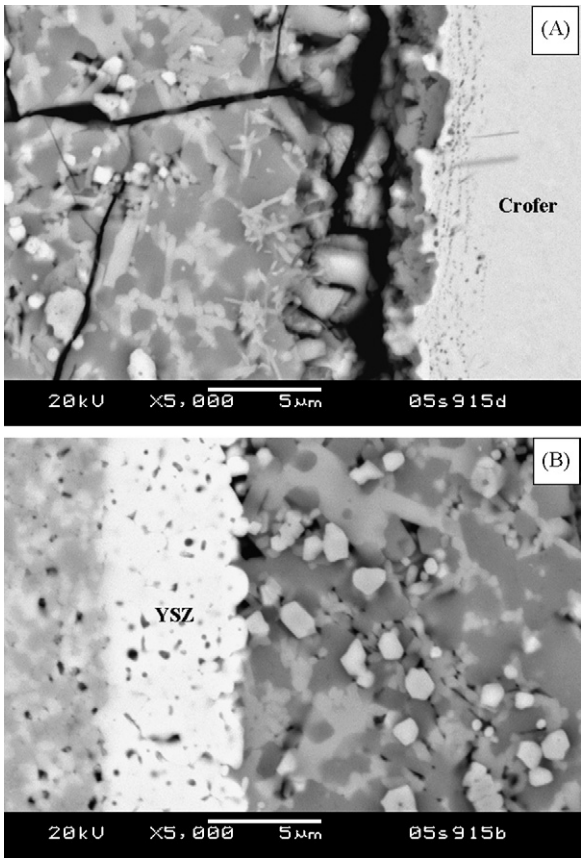

Fig. 4. Interfacial microstructure of composite glass (YSO-15) sealed at 1050 °C/2 h at (A) Crofer metal and (B) YSZ electrolyte interface.

At the glass/metal interface, there appeared two or three distinct layers for samples sealed at 950, 1000, and 1050 °C (Figs. 2A, 3A, and 4A, respectively). Samples sealed at 1000 °C (Fig. 3A) showed the most clear and different morphology of these layers. The layer next to base metal is a Cr-based oxide layer (#1 in Fig. 3A) about 1 μm thick, and appeared discrete and non-uniform in thickness. The Cr-based oxide layers were slightly thinner for samples sealed at 950 °C and slightly thicker for 1050 °C. The bare metal; however, showed a thicker and more uniform oxide layer (#1 in Fig. 5A) where no sealing glass was applied. Next to the Cr-based oxide layer, there was a small band with different morphology of finer precipitate (#2 in Fig. 3A) which was found to be Cr-based oxides with appreciable amount of Ni, as well as Fe and Mn (elemental analyses corresponding to these spots (#1–5 in Fig. 3A are listed in Table 3). This layer was not clear to identify for samples sealed at 950 and 1050 °C. Spot #3 contained crystallized $SrSiO_3$ with small amounts of Cr from the surroundings. Spot #4 contained primarily Cr and Sr in atomic ratio close to 1:1 and was believed to be $SrCrO_4$. This layer was more evident for samples sealed at 950 and 1050 °C. Spot #5 was a silicate with Sr and Y. The bulk microstructure of the crystallized glass was clearer in Fig. 3B, consisting of dark grains (#3) and light grains (#5) with evenly distributed NiO spherical particles.

It's interesting to note that there appeared to be a depletion zone, about 10–15 μm, of NiO particle near the glass/metal interface (Figs. 2A, 3A, and 4A). For comparison, the NiO particles were more evenly distributed along or near the glass/YSZ interface and within the bulk of glass (Fig. 3B). The band with finer precipitates (spot#2 in Fig. 3A) contained appreciable amounts of Ni (~14 at.%) as well as Cr (~28 at.%) and Fe (~7 at.%) (Table 3). Calculation of Gibbs free energy for the following reactions was therefore performed for two temperatures (maximum sealing of 1050 °C and crystallization of 800 °C):

$$NiO + Mn_2O_3 \rightarrow NiMn_2O_4,$$
$$\Delta G = 180\,\text{kJ mol}^{-1}\,(800\,^\circ\text{C}),\ 243\,\text{kJ mol}^{-1}\,(1050\,^\circ\text{C}) \quad (1)$$

Table 3
Elemental analysis of spots in the as-sealed coupons of Fig. 3A

Atom%	#1	#2	#3	#4	#5
O	38.57	41.89	45.83	50.5	45.7
Si	1.01	2.38	22.17	2.13	19.15
Ca	0.23	0.92	2.98	0.44	6.21
Ti	0.33				
Cr	43.01	28.59	5.79	23.27	
Mn	0.79	2.58			
Fe	12.78	6.87	0.71	0.54	
Ni	1.71	14.3	0.94	1.16	1.64
Br	1.19	1.69			
Sr	0.39		21.57	21.96	13.96
Y		0.78			13.34

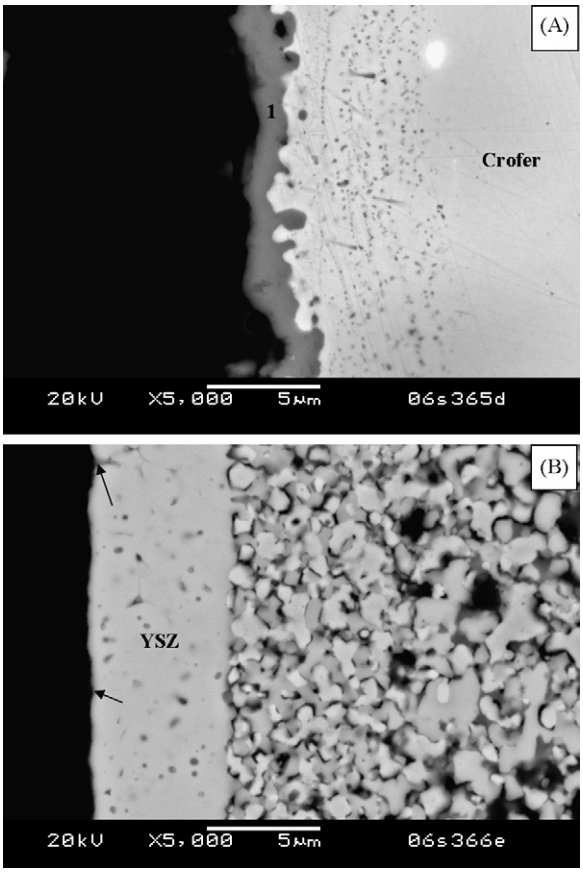

Fig. 5. Microstructure of bare Crofer and YSZ without sealing glass taken through the same heat-treatment as the sealed coupons. Point #1 in (A) shows the Cr_2O_3-based oxide layer and arrows in (B) show the smooth YSZ surface with less evidence of grain boundary grooving.

$$NiO + Fe_2O_3 \rightarrow NiFe_2O_4,$$
$$\Delta G = -24\,\text{kJ mol}^{-1}\,(800\,^\circ\text{C}),\ -27\,\text{kJ mol}^{-1}\,(1050\,^\circ\text{C}) \quad (2)$$

$$NiO + Cr_2O_3 \rightarrow NiCr_2O_4,$$
$$\Delta G = -8\,\text{kJ mol}^{-1}\,(800\,^\circ\text{C}),\ -9\,\text{kJ mol}^{-1}\,(1050\,^\circ\text{C}) \quad (3)$$

It was reported that the oxidation of crofer in air often resulted in two oxide scales. The inner thick layer formed first and was primarily Cr_2O_3. The outer layer involved the diffusion of Mn and therefore formed later and thinner, and was often identified as $(Mn,Cr)_3O_4$ spinel. In our short heat-treatment (800 °C/4 h for crystallization) no distinctive layer of $(Mn,Cr)_3O_4$ spinel was identified, and no thermodynamic data was available. The Gibbs free energy calculations were therefore limited to single oxides. The negative Gibbs free energies of Eqs. (2) and (3) suggest that NiO particles migrated toward the metal interface and reacted with the oxide layer (rich in Cr and Fe). The elemental analyses showed an atomic ratio of approximately 1:2 for Ni:Cr seems to suggest reaction 3 was more dominant, though reaction (2) was more negative in Gibbs free energy. This is likely related to the higher activity of chromium oxide than the iron oxide as evidenced by the oxide layer was primarily Cr_2O_3 when the metal was exposed in air at elevated temperatures.

3.3. Interfacial characterization of as-sealed coupons along YSZ/glass interface

As for the glass/YSZ interface, no distinct morphology along the interface was found, suggesting minimal reaction of YSZ with the glass. However, the YSZ grains showed pronounced grain boundary grooving (arrows in Fig. 3B) as compared to the bare YSZ electrolyte without the sealing glass (Fig. 5B). The enhanced grain boundary grooving was likely due to the presence of molten sealing glass at sealing temperatures which provided a fast transport path for the thermally activated diffusion process. Reaction between Sr-silicate and YSZ was not thermodynamically favorable in the temperature range since the calculated Gibbs free energy was positive:

$$SrSiO_3 + ZrO_2 \rightarrow SrZrO_3 + SiO_2,$$
$$\Delta G = 51\,\text{kJ mol}^{-1}\,(800\,^\circ\text{C}),\ 49\,\text{kJ mol}^{-1}\,(1050\,^\circ\text{C}) \quad (6)$$

3.4. Interfacial characterization of fully reduced coupons

As for the fully reduced and thermally cycled coupons, the interfacial microstructure is shown in Fig. 6A and B for the glass/metal interface and glass/YSZ interface, respectively. The microstructure at the interface and in the bulk glass was very

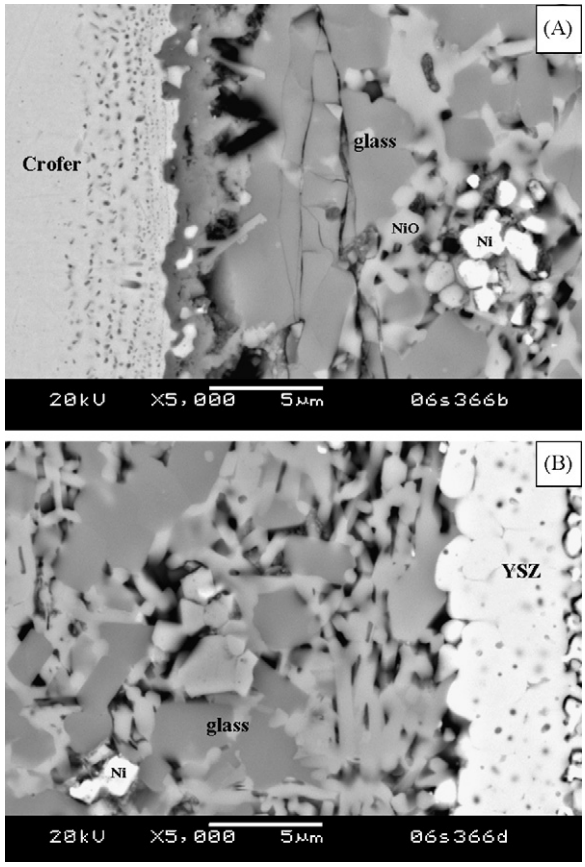

Fig. 6. Interfacial microstructure of the reduced and thermally cycled coupons using composite glass (YSO-15): (A) glass/metal interface, and (B) glass/YSZ interface. The darker phase (#1) in (B) was $SrSiO_3$ and the lighter phase (#2) was a silicate rich in Sr and Y.

similar to the as-sealed coupons with the darker $SrSiO_3$ phase (#1 in Fig. 6B) and a lighter silicate phase rich in Sr and Y (#2 in Fig. 6B). However, some of the NiO particles appeared to be reduced to metal Ni (white particles in Fig. 6A and B), while others remained as oxide. It was also noted that no strontium chromate ($SrCrO_4$) was found along the metal interface. This phase is undesirable due to its very high CTE, $\sim 22 \times 10^{-6}\,^{\circ}C^{-1}$ average from room temperature to 1000 °C [21]. At the presence of oxygen, $SrCrO_4$ can be formed by the following reactions:

$$SrO + (1/2)Cr_2O_3 + (3/4)O_2 = SrCrO_4 \quad (7)$$

$$SrSiO_3 + (1/2)Cr_2O_3 + (3/4)O_2 = SrCrO_4 + SiO_2 \quad (8)$$

However, in the reducing environment, the formation $SrCrO_4$ was expected to be thermodynamically unfavorable. A study of chemical compatibility by Yang et al. of a similar glass (Ba–Ca–Al–B–Si) with ferritic stainless steel interconnect material showed positive Gibbs free energy for barium chromate formation at $T > 700\,^{\circ}C$ in reducing environment ($P_{O_2} = 10^{-16}$ atm). [18].

4. Summary and conclusions

A novel Sr-silicate sealing glass for SOFC was developed with a focus on the effects of NiO on thermal, mechanical, and interfacial reactions. A composite approach was used to study the interfacial reaction and microstructure in part II. Coupon sealing was conducted at three sealing temperatures with the 10 vol.% NiO composite glass. Leakage test results showed hermetic seals for samples sealed at 1050 °C including the reduced and thermally cycled seals. Interfacial microstructure and chemical analysis were conducted to address the potential interfacial reactions. At YSZ interface, the glass composite appeared to be stable without undesirable phase formation. At the metal interface; however, $SrCrO_4$ was found and some Ni segregation was identified. Overall, the composite glass approach with NiO demonstrated a viable way to tailor thermal and mechanical properties of candidate SOFC sealing glasses.

Acknowledgements

The authors would like to thank S. Carlson and J. Coleman for SEM sample preparation and analysis. This paper was funded as part of the Solid-State Energy Conversion Alliance (SECA) Core Technology Program by the US Department of Energy's National Energy Technology Laboratory (NETL). Pacific Northwest National Laboratory is operated by Battelle Memorial Institute for the US Department of Energy under Contract no. DE-AC06-76RLO 1830. Robert Gow would also like to acknowledge the U.S. DOE, Office of Science's Community College Initiative, CCI Program, his mentor, Dr. Yeong-Shyung Chou, and other PNNL employees for their help during his summer internship.

References

[1] N.Q. Minh, J. Am. Ceram. Soc. 76 (3) (1993) 563–588.
[2] Y.S. Chou, J.W. Stevenson, J. Power Sources 125 (2004) 72–78.
[3] X. Qi, F.T. Akin, Y.S. Lin, J. Membr. Sci. 193 (2001) 185–193.
[4] S. Taniguchi, M. Kadowaki, T. Yasuo, Y. Akiyama, Y. Miyake, K. Nishio, J. Power Sources 90 (2000) 163–169.
[5] K.L. Ley, M. Krumpelt, R. Kumar, J.h. Meiser, I. Bloom, J. Mater. Res. 11 (6) (1996) 1489–1493.
[6] V.A.C. Haanappel, V. Shemet, I.C. Vinke, S.M. Gross, T.H. Koppitz, N.H. Menzler, M. Zahid, W.J. Quadakkers, J. Mater. Sci. 40 (2005) 1583–1592.
[7] N. Lahl, D. Bahadur, K. Singh, L. Singheiser, K. Hilpert, J. Electrochem. Soc. 149 (5) (2002) A607–A614.
[8] N. Lahl, K. Singh, L. Singheiser, K. Hilpert, D. Bahadur, J. Mater. Sci. 35 (2000) 3089–3096.
[9] S.-B. Sohn, S.-Y. Choi, G.-H. Kim, H.-S. Song, G.-D. Kim, J. Non-Crystal. Solids 297 (2002) 103–112.
[10] P.H. Larsen, P.F. James, J. Mater. Sci. 33 (1998) 2499–2507.
[11] Z. Yang, J.W. Stevenson, K.D. Meinhardt, Solid State Ionics 160 (2003) 213–225.
[12] Y.S. Chou, J.W. Stevenson, J. Power Sources 112 (2002) 376–383.
[13] Y.S. Chou, J.W. Stevenson, J. Power Sources 140 (2005) 340–345.
[14] K.S. Weil, J.S. Hardy, J.Y. Kim, Use of a novel ceramic-to-metal braze for joining in high temperature electrochemical devices, J. Adv. Specialty Mater. V: Am. Soc. Met. 5 (2000) 47–55.
[15] J. Duquette, A. Petric, J. Power Sources 137 (2004) 71–75.
[16] K.S. Weil, J.Y. Kim, J.S. Hardy, Electrochem. Solid State Lett. 8 (2005) A133–A136.
[17] K.D. Meinhardt, L.R. Pederson, US Patent 6,430,966 (2002).
[18] Z. Yang, K.D. Meinhardt, J.W. Stevenson, J. Electrochem. Soc. 150 (8) (2003) A1095–A1101.
[19] V.A.C. Haanappel, V. Shemet, S.M. Gross, Th. Koppitz, N.H. Menzler, M. Zahid, W.J. Quadakkers, J. Power Sources 150 (2005) 86–100.
[20] Y.-S. Chou, J.W. Stevenson, R.N. Gow, Novel alkaline earth silicate sealing glass for SOFC. Part I. The effect of NiO on the thermal and mechanical properties, J. Power Sources (2007).
[21] Y. S. Chou, J.W. Stevenson, Unpublished work.